CAPEX Study for a Multilayer IP/MPLS-Over-Flexgrid Optical Network

O. Pedrola, A. Castro, L. Velasco, M. Ruiz, J. P. Fernández-Palacios, and D. Careglio

***Abstract*—The ever-increasing Internet Protocol (IP) traffic volume has finally brought to light the high inefficiency of current wavelength-routed over rigid-grid optical networks in matching the client layer requirements. Such an issue results in the deployment of large-size, expensive, and power-consuming IP/Multi-Protocol Label Switching (MPLS) layers to perform the required grooming/aggregation functionality. To deal with this problem, the emerging flexgrid technology, allowing for reduced-size frequency grids (usually referred to as frequency slots), has recently attracted much attention among network operators, component and equipment suppliers, and the research community. In this paper, we tackle the multilayer IP/MPLS-over-flexgrid optimization problem. To this end, an integer linear programing formulation and a greedy randomized adaptive search procedure (GRASP) metaheuristic are provided. Using GRASP, we analyze the cost implications that a set of frequency slot widths have on the capital expenditure investments required to deploy such a multilayer network. For the sake of a compelling analysis, exhaustive numerical experiments are carried out considering a set of realistic network topologies, network equipment costs, and traffic instances. Results show that investments in optical equipment capable of operating under slot widths of 12.5 GHz, or even 25 GHz, are more appropriate, given the expected traffic evolution.**

***Index Terms*—Flexgrid optical networks; Metaheuristic algorithms; Multilayer network planning; Network optimization.**

I. Introduction

The dramatic increase in the use of new disruptive bandwidth-intensive services and applications has led to a huge surge of Internet Protocol (IP) traffic, which ultimately has brought to light the clear granularity mismatch between the client layer and the current wavelength-routed dense-wavelength-division-multiplexing (DWDM-) based optical layer. This issue results in a highly inefficient use of the network capacity and consequently in multilayer networks requiring a large amount of highly expensive power-consuming IP/Multi-Protocol Label Switching (MPLS) equipment to be installed for aggregation (at the edge) and grooming (at the intermediate nodes) purposes.

In this context, flexgrid technology [1,2] provides higher spectrum efficiency and flexibility in comparison to a traditional wavelength-switched optical network (WSON). By leveraging key advances in optical multi-level modulation techniques and the design of both bandwidth-variable transponders (BV-Ts) and bandwidth-variable wavelength selective switches (BV-WSSs), the main components enabling the design of bandwidth-variable wavelength cross-connects (BV-WXCs), flexgrid optical networks are able to provide both sub- and super-wavelength traffic accommodation. Whilst BV-Ts may work under both single- and multi-carrier advanced modulation formats such as quadrature phase-shift keying (QPSK), quadrature amplitude modulation (QAM), and optical orthogonal frequency division multiplexing (O-OFDM) [2], BV-WXCs can be assembled using existing devices such as the *WaveShaper* programmable optical processor [3]. Thanks to this flexible technology, a flexgrid optical network can adjust to varying traffic conditions over time, space, and bandwidth, thereby creating a network scenario in which wavelength channels are both switched and dimensioned (bit-rate/reach/signal bandwidth) according to temporary traffic requirements.

To this end, flexgrid optical networks divide the available optical spectrum into a set of frequency slots (FSs) of a fixed finer spectral width in comparison to the current ITU-T DWDM rigid frequency grid (50 GHz) [4]. Current proposals for the slot size are 25 GHz, 12.5 GHz, and 6.25 GHz, the latter two being mentioned in the industry as potential minimum bandwidth granularities. Therefore, traffic demands are assigned a given number of FSs according to their requested bit-rate, the selected modulation technique, and the considered frequency grid (i.e., the slot width) [2].

Consequently, in this flexible and dynamic network scenario, the classic constraints found in wavelength-routed networks, which are dealt with by routing and wavelength assignment algorithms, are not applicable anymore. Specifically, in flexgrid optical networks there emerges the so-called routing and spectrum assignment (RSA) problem, in which spectrum continuity along the links in the route of a given path (i.e., the same slots must be used in all the links of the path) as well as spectrum contiguity (i.e., the slots must be contiguous in the spectrum) must be guaranteed [5]. This problem poses new challenges for the design of future flexgrid optical networks and thus has rapidly aroused great interest within the research community. For instance, some recent works tackle the RSA problem for either the static/off-line (traffic demands are known a priori) [5–7] or the dynamic/on-line (connection requests are provisioned upon their arrival)

Manuscript received March 26, 2012; revised June 12, 2012; accepted July 7, 2012; published August 1, 2012 (Doc. ID 165402).

O. Pedrola (e-mail: opedrola@ac.upc.edu) is with the Advanced Broadband Communications Center (CCABA), Universitat Politècnica de Catalunya (UPC), Barcelona, Spain, and is also with the Department of Electrical Engineering, Columbia University, New York, New York 10027, USA.

A. Castro, L. Velasco, M. Ruiz, and D. Careglio are with the Advanced Broadband Communications Center (CCABA), Universitat Politècnica de Catalunya (UPC), Barcelona, Spain.

J. P. Fernández-Palacios is with Telefónica I+D, Madrid, Spain.

Digital Object Identifier 10.1364/JOCN.4.000001

network scenario [8,9]. The study and development of complex RSA models and algorithms is nevertheless out of the scope of this work. In fact, here we make use of both a simplified RSA integer linear programing (ILP) model proposed in [7], which removes spectrum contiguity constraints by pre-computing demand-tailored channels (sets of spectrum contiguous slots), and an efficient RSA strategy similar to the fixed-alternate and first-fit frequency allocation algorithm proposed in [2] and evaluated in [10].

Our goal in this paper is, by contrast, to analyze, for a number of candidate slot widths, the capital expenditure (CAPEX) needed to deploy a multilayer IP/MPLS-over-flexgrid architecture. To this end, we model the multilayer IP/MPLS-over-flexgrid optimization problem (hereinafter referred to as the MIFO problem) by means of both an ILP formulation and a greedy randomized adaptive search procedure (GRASP) algorithm and solve it considering a range of real-sized network and traffic instances. GRASP is an iterative two-phase metaheuristic method based on a multi-start randomized search technique. Over the years, GRASP models have been used to solve a wide range of problems with many and varied applications in real life, such as the design of communication networks and medical image registration [11–13]. For a recent and comprehensive survey of GRASP, the reader is referred to [14].

It is clear that finer grids will allow for more efficient spectrum utilization and as a result favor grooming data directly at the optical layer instead of requiring costly IP/MPLS equipment for such functionality. Thus, given the fact that the network CAPEX, that is, those costs related to purchasing and installing fixed infrastructures, is a figure network operators are always striving to reduce, the introduction of flexgrid technology is of paramount importance for future multilayer networks [15]. However, it must be noted that while reducing the need for grooming at the IP/MPLS layer, this more advanced optical technology will also imply higher costs at the optical layer given the highly demanding (grid-dependent) filtering characteristics that BV-WSSs are required to have. In addition, due to the increased spectrum fragmentation (particularly for the 12.5 GHz and 6.25 GHz grids), more complex network management, and therefore more advanced control planes, will be required, thereby leading to cost increases. Since the exact costs for such components are still not available, in this study we consider a relative cost value to approximately quantify both these additional costs and, by this means, effectively determine which frequency grid will better address a network operator's needs for cost-effective, spectrum-efficient network architectures.

The rest of this paper is organized as follows. Section II details the MIFO problem. Section III presents an ILP formulation which provides insight into the complexity of managing MIFO under realistic conditions. Given its complexity, in Section IV, a GRASP metaheuristic specifically tailored to solve MIFO is presented. Illustrative numerical results are provided in Section V, and Section VI concludes the paper.

II. Multilayer IP/MPLS-Over-Flexgrid Optimization Problem

In the literature, the multilayer network optimization problem has been tackled with a variety of objectives (see, e.g., [16–21]). In fact, each time a novel optical transport technology emerges, such a problem has to be redefined. For example, in [20], the authors propose heuristics to minimize CAPEX for a multilayer network based on a synchronous digital hierarchy over static point-to-point DWDM. More recently, in [16], the authors deal with the survivable multilayer IP/MPLS-over-WSON optimization problem. Nowadays, the innovation is the replacement of the WSON technology with the emerging flexgrid paradigm. The aim of the MIFO problem is to effectively exploit network resources while, at the same time, minimizing CAPEX investments. This fact inevitably sets our focus on the size of the costly electronic layer, and hence on the reduction of IP/MPLS equipment.

As aforementioned, flexgrid optical networks divide the available optical spectrum into a set of FSs. Then, the number of FSs each traffic demand is assigned depends on the network slot width (sw), the demand bit-rate (b_d), and the number of bits/symbol that the modulation format is able to carry (B_{mod}). Note that B_{mod} determines both the spectral efficiency of the modulation format (bits/s/Hz) and the symbol rate, and consequently the spectral bandwidth required to transmit the signal [2]. Hence, at a given fixed data rate, spectral savings can be obtained by reducing the symbol rate (i.e., increasing B_{mod}). For example, under good channel conditions, an advanced modulation format such as 64-QAM ($B_{\text{mod}} = 6$) would only require 1/3 of the spectral bandwidth used if QPSK ($B_{\text{mod}} = 2$) was used instead. However, these improvements come at the cost of reducing the optical path lengths, as higher B_{mod} implies higher signal to noise ratio penalties and worse receiver sensitivity [2].

In order to estimate the number of FSs (n_d) (i.e., spectral bandwidth) that each traffic demand will require, we suggest using the following formula, which is in line with [2]:

$$n_d = \left\lceil \frac{b_d}{sw \cdot B_{\text{mod}}} \right\rceil. \tag{1}$$

It must be mentioned that Eq. (1) tends to underestimate the number of FSs required, as it assumes that b_d consists only of payload data. However, in general, this is not the case, as different overhead data (e.g., around 10% extra) may be required. Such overhead may vary according to the modulation format selected. For instance, in OFDM-based systems, overhead symbols are required to avoid inter-symbol interference. Additionally, the selection of the modulation format may depend on each particular demand bit-rate. These issues, however, are out of the scope of this work.

Specifically, in this paper, we consider QPSK ($B_{\text{mod}} = 2$) as the modulation format for all traffic demands, which are assumed to be of 10, 40, 100, or 400 Gb/s each. This way, the focus is set on the evaluation of the CAPEX savings that can be achieved through the use of narrower slot widths. Using Eq. (1), Table I reports the number of FSs that each demand requires under the different slot widths evaluated. One can observe that, under the 50 GHz grid, 10, 40, and 100 Gb/s

TABLE I
FSs Required per Demand Under Each Frequency Grid

Demand (Gb/s)	10	40	100	400
$sw = 50$ GHz	1	1	1	4
$sw = 25$ GHz	1	1	2	8
$sw = 12.5$ GHz	1	2	4	16
$sw = 6.25$ GHz	1	4	8	32

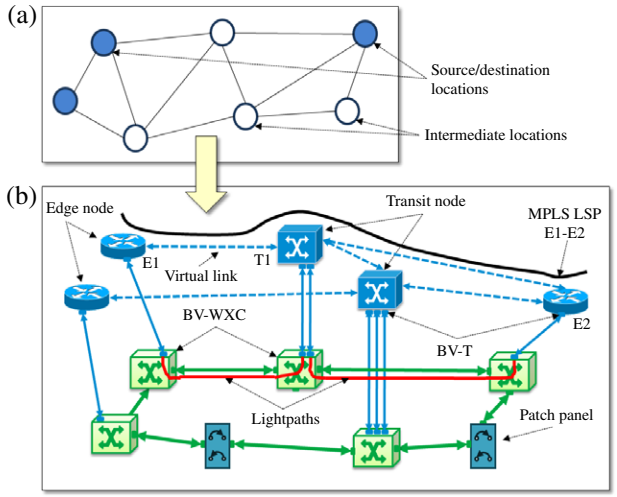

Fig. 1. (Color online) (a) Geographical distribution for network topology locations. In blue, nodes that are the source/destination of IP/MPLS traffic demands. White circles represent candidate locations where network equipment can be installed if necessary. (b) A multilayer network illustrating a possible solution for the MIFO problem.

demands will require the same number of FSs, that is, 1. However, under a 6.25 GHz grid, the same set of demands would need, respectively, 1, 4, and 8 FSs, thereby clearly illustrating the spectrum efficiency that can be obtained using finer BV-WSSs at the optical layer.

Note also that the demand to FS mapping shown in Table I not only has an impact on the spectral efficiency achieved, but also on the number and type of the BV-Ts deployed. In this work, the grooming of demands into lightpaths aims at minimizing the number of FSs used. Hence, considering the type and BV-T costs provided in Section V.A, two demands of 10 Gb/s, following the same path, would be groomed into a 40 Gb/s lightpath (requiring one 40 Gb/s BV-T at each end) in both the 50 GHz and 25 GHz grids. On the other hand, in both the 12.5 GHz and 6.25 GHz grids, two 10 Gb/s lightpaths (two 10 Gb/s BV-Ts at each end) would be set up. Note that in the 12.5 GHz grid the tie in the number of FSs is broken by selecting the cheapest option, which in this case is two 10 Gb/s BV-Ts. According to this discussion, it can be anticipated that networks using finer slot widths will feature a larger number of BV-Ts but with a considerably lower average bit-rate.

In order to tackle MIFO, we assume that a network topology representing a set of geographical locations as well as the interconnectivity among them (i.e., the fibers are already deployed) is given in advance. In these sites, network equipment can be installed if necessary (see Fig. 1(a)). Moreover, we assume that only a limited number of locations can be the source/destination of IP/MPLS demands (blue locations). As required, nodes are equipped with BV-Ts so as to provide connectivity between the electronic and optical layers. The remaining locations (intermediate locations) are candidate spots where network equipment is installed according to the functionality required. Specifically, and given a set of traffic demands to be accommodated, intermediate locations can be either (1) a multilayer node with both IP/MPLS and BV-WXC functionality, (2) a BV-WXC node if no IP/MPLS operation is required, (3) a patch panel connecting optical fibers if neither IP/MPLS nor BV-WXC is required at such location, or (4) an empty location if no demand traverses such location. In Fig. 1(b), a multilayer network exemplifying a possible solution to the MIFO problem applied to the topology of Fig. 1(a) is shown. One can observe locations that are equipped with multilayer nodes providing either client flow aggregation (edge nodes) or routing flexibility (transit nodes). Other locations, however, only operate as patch panels for fiber connectivity purposes, thereby minimizing the network CAPEX.

As an example, Fig. 1(b) illustrates one of the MPLS label-switched paths (LSPs) established in the network, that is, LSP E1–E2. In this case, this LSP entails tearing up two lightpaths to support virtual links E1–T1 and T1–E2. Recall that one lightpath, which is associated with two BV-Ts (one at each end), can be used to transport several traffic demands and, by this means, provide the grooming functionality required to optimize the use of network resources. It is worth pointing out that the solution obtained by solving the MIFO problem (i.e., the location, type, and quantity of network equipment deployed) will vary in accordance with the input traffic demands considered.

In the next section, first the MIFO problem is formally stated, and second an ILP-based formulation of the problem is provided.

III. Mathematical Formulation

A. MIFO Problem Statement

The MIFO problem can be formally stated as follows.

Given:

- A network topology represented by a graph $G_o(V,L)$, with V being the set of locations and L the set of bidirectional fiber links connecting two locations; each link consists of two unidirectional optical fibers.
- A set S of available frequency slots of a given spectral width in each link in L.
- The virtual network represented by a graph $G_v(V_v,E)$, with V_v being the subset of locations V where IP/MPLS nodes can be placed and E the set of virtual links defining the connectivity among the IP/MPLS locations.
- A set D of IP/MPLS demands to be transported.
- The IP/MPLS equipment cost, specified by a fixed cost for every type of IP/MPLS node and BV-T.
- The cost of the BV-WXC nodes, which includes a fixed cost for the base system and a variable cost as a function of the

nodal degree including the cost of BV-WSSs (note that the relevant nodal degree, i.e., the number of incident links, is that of the final solution). See Fig. 4 in [1] for further details on the BV-WXC architecture.

- A cost for every intermediate optical amplifier to be equipped in the fiber links and a cost per km and GHz for using the deployed fiber. It should be emphasized that the fiber costs considered in this work only relate to its use, and not to its deployment. Consequently, the cost per spectral bandwidth is also accounted for to have a better estimation of the cost of the fiber resources used. Note that, if only half of the spectral bandwidth of a given fiber is used, the remaining free capacity can be rented to other clients.

Output:

- The optical network, including patch panels, optical nodes with the number of optical interfaces, and the used fiber links.
- The configuration of IP/MPLS nodes in terms of the capacity and the number and bit-rate of the BV-Ts.

Objective: minimize the total CAPEX of the designed multilayer network for the given set of demands.

The problem can be tackled by solving the following ILP model.

B. ILP Model

The ILP model for the MIFO problem designs both the optical and the IP/MPLS layers using two node-link formulations [21], that is, one per network layer. Note that, although the link-path formulation could be used for the optical layer, the number of routes to be pre-computed should be large enough to overcome the fact that some locations would not be equipped in the optimal solution. Instead, we compute a set of virtual links connecting every pair of locations where IP/MPLS nodes can be installed. For each virtual link, a set of lightpaths is available, but its route on the optical topology is determined during the resolution of the problem.

As to how the spectrum allocation is performed, channels are used to ensure frequency slot contiguity in the input data [7], thereby alleviating to some extent the problem complexity. The characteristics of the considered modulation format are also embedded in the input data. To be precise, the slot's capacity in Gb/s is pre-computed (parameter sk) and different optical signal reaches (parameter len(r)) as a function of both the bit-rate and modulation format are considered. Aiming at simplifying the dimensioning of the IP/MPLS nodes, a set of port slots is available at each location. The solution of the problem provides the characteristics of the specific BV-T installed in each port slot, if any.

The following sets and parameters have been defined.

Topology:

V	Set of locations, index v.
L	Set of fiber links, index l.
len(l)	Length of fiber link l in km.
$L(v)$	Subset of fiber links incident to location v.
V_v	Set of locations where IP/MPLS nodes can be placed.
E	Set of virtual links, index e.
$K(e)$	Set of lightpaths to support virtual link e, index k.
$E(v)$	Subset of virtual links incident to node v.
$V(e)$	Set of end nodes of virtual link e.
$P(v)$	Set of port slots of location v, index p.
as	Amplifier span for fiber links in kilometers.

Spectrum and modulation formats:

S	Set of frequency slots, index s.
sw	Frequency slot width in GHz.
sk	Frequency slot capacity in Gb/s.
C	Set of channels, index c. Each channel c contains a subset of contiguous frequency slots.
n^c	Number of frequency slots included in channel c.
h_s^c	Equal to 1 if channel c includes frequency slot s, 0 otherwise.
R	Set of bit-rate-reach pairs (Gb/s, km), index r.
len(r)	Reach of a lightpath using bit-rate-reach pair r in km.
$bw(r)$	Maximum bit-rate of a lightpath using bit-rate-reach pair r in Gb/s.

Demands:

D	Set of IP/MPLS demands, index d.
$SD(d)$	Set of source and destination nodes of demand d.
b_d	Bandwidth of demand d in Gb/s.

Equipment, costs, and others:

NT	Set of node types, index n (Patch, BV-WXC, IP/MPLS). Note that type IP/MPLS includes one BV-WXC.
C_{WXC}	Fixed cost of one BV-WXC. Includes common circuitry and BV-WSSs.
C_{FO}	Cost per km and GHz of using the optical fiber.
C_{Trunk}	Cost of one trunk, which includes one BV-WSS, one optical amplifier, and one optical splitter.
$\max\varphi$	Maximum optical nodal degree (number of trunks) of a BV-WXC.
C_{OA}	Cost of each intermediate optical amplifier.
RT	Set of IP/MPLS node classes, index j. Each class defined by a switching capacity and a number of BV-T slots.
rk_j	Switching capacity of an IP/MPLS node class j in Gb/s.
rpk_j	Number of BV-T port slots available in an IP/MPLS node class j.
rc_j	Cost of one IP/MPLS node of class j.
PT	Set of BV-T bit-rates, index i.
pk_i	Capacity of a BV-T of bit-rate i in Gb/s.
mpc_i	Cost of one BV-T of bit-rate i in an IP/MPLS node.
M	A large positive constant.

The decision variables are as follows.

ω_{dek}	Binary. Equal to 1 if demand d is routed through lightpath k of virtual link e, 0 otherwise.

δ^c_{ek} Binary. Equal to 1 if lightpath k of virtual link e uses channel c, 0 otherwise.

λ^c_{ekl} Binary. Equal to 1 if lightpath k of virtual link e uses channel c in fiber link l, 0 otherwise.

γ_l Binary. Equal to 1 if fiber link l is used, 0 otherwise.

$\sigma^{e'k'}_{ekl}$ Binary. Equal to 1 if lightpath k of virtual link e and lightpath k' of virtual link e' share fiber link l, 0 otherwise.

Ψ^{vp}_{ek} Binary. Equal to 1 if lightpath k of virtual link e is assigned to port slot p in location v, 0 otherwise.

φ^v Positive integer with the optical nodal degree of location v.

ρ^{vp}_i Binary. Equal to 1 if port slot p of location v is equipped with a BV-T of bit-rate i, 0 otherwise.

π^v_j Binary. Equal to 1 if location v is equipped with an IP/MPLS node of class j, 0 otherwise.

μ^v_n Binary. Equal to 1 if location v is equipped with a node type n, 0 otherwise.

τ^{vp} Positive integer with the total amount of traffic (in Gb/s) using port slot p of location v.

ν^r_{ek} Binary. Equal 1 if lightpath k of virtual link e uses bit-rate-reach pair r.

α^v Positive real with the optical cost of location v.

β^v Positive real with the IP/MPLS cost of location v.

Then, network CAPEX can be computed as the sum of the following expressions:

$$\mathrm{COST}_{\mathrm{Equipment}} = \sum_{v\in V}(\alpha^v+\beta^v), \tag{2}$$

$$\mathrm{COST}_{\mathrm{FO}} = \sum_{l\in L}\gamma_l\cdot\left\lceil\left(\frac{\mathrm{len}(l)}{as}-1\right)\right\rceil\cdot C_{\mathrm{OA}} + \sum_{l\in L}\sum_{c\in C}\sum_{e\in E}\sum_{k\in K(e)}\lambda^c_{ekl}\cdot n_c\cdot sw\cdot\mathrm{len}_l\cdot C_{\mathrm{FO}}, \tag{3}$$

where Eq. (2) computes the cost of the nodes and BV-T ports, and Eq. (3) the cost of the optical fiber as a result of both installing intermediate optical amplifiers and using the fiber links.

Finally, the ILP for the MIFO problem is as follows.

MIFO:

$$\text{minimize CAPEX} = \mathrm{COST}_{\mathrm{Equipment}} + \mathrm{COST}_{\mathrm{FO}} \tag{4}$$

subject to:

$$\sum_{e\in E(v)}\sum_{k\in K(e)}\omega_{dek} = 1, \quad \forall d\in D, v\in SD(d), \tag{5}$$

$$\sum_{e\in E(v)}\sum_{k\in K(e)}\omega_{dek} \le 2, \quad \forall d\in D, v\in \overline{SD(d)}, \tag{6}$$

$$\sum_{\substack{e\in E(v)\\ e'\neq e}}\sum_{k\in K(e')}\omega_{de'k} \ge \sum_{k\in K(e)}\omega_{dek}, \quad \forall d\in D, v\in\overline{SD(d)}, e\in E(v), \tag{7}$$

$$\sum_{l\in L(v)}\sum_{c\in C}\lambda^c_{ekl} = \sum_{c\in C}\delta^c_{ek}, \quad \forall e\in E, k\in K(e), v\in V(e), \tag{8}$$

$$\sum_{l\in L(v)}\sum_{c\in C}\lambda^c_{ekl} \le 2, \quad \forall e\in E, k\in K(e), v\in\overline{V(e)}, \tag{9}$$

$$\sum_{\substack{l'\in L(v)\\ l'\neq l}}\sum_{c\in C}\lambda^c_{ekl'} \ge \sum_{c\in C}\lambda^c_{ekl}, \quad \forall e\in E, k\in K(e), v\in\overline{V(e)}, l\in L(v), \tag{10}$$

$$\sum_{c\in C}\delta^c_{ek} \le 1, \quad \forall e\in E, k\in K(e), \tag{11}$$

$$\sum_{c\in C} sk\cdot n^c\cdot\delta^c_{ek} \ge \sum_{d\in D} b_d\cdot\omega_{dek}, \quad \forall e\in E, k\in K(e), \tag{12}$$

$$\sum_{l\in L}\lambda^c_{ekl} \le M\cdot\delta^c_{ek}, \quad \forall e\in E, k\in K(e), c\in C, \tag{13}$$

$$\sum_{e\in E}\sum_{k\in K(e)}\sum_{c\in C} h^c_s\cdot\lambda^c_{ekl} \le 1, \quad \forall l\in L, s\in S, \tag{14}$$

$$\sum_{d\in D} b_d\cdot\omega_{dek} \le \sum_{r\in R} bw(r)\cdot\nu^r_{ek}, \quad \forall e\in E, k\in K(e), \tag{15}$$

$$\sum_{l\in L}\sum_{c\in C}\mathrm{len}(l)\cdot\lambda^c_{ekl} \le \sum_{r\in R}\mathrm{len}(r)\cdot\nu^r_{ek}, \quad \forall e\in E, k\in K(e), \tag{16}$$

$$\sum_{r\in R}\nu^r_{ek} \le 1, \quad \forall e\in E, k\in K(e), \tag{17}$$

$$\sum_{e\in E}\sum_{k\in K(e)}\sum_{c\in C}\lambda^c_{ekl} \le M\cdot\gamma_l, \quad \forall l\in L, \tag{18}$$

$$\sum_{l\in L(v)}\gamma_l = \varphi^v, \quad \forall v\in V, \tag{19}$$

$$\varphi^v \le M\cdot\sum_{n\in\mathrm{NT}}\mu^v_n, \quad \forall v\in V, \tag{20}$$

$$\sum_{n\in\mathrm{NT}}\mu^v_n \le 1, \quad \forall v\in V, \tag{21}$$

$$\varphi^v \le \max\varphi + M\cdot\mu^v_n, \quad \forall v\in V, n\in\{\mathrm{Patch}\}, \tag{22}$$

$$\sum_{d\in D}\sum_{k\in K(e)}\omega_{dek} \le M\cdot\mu^v_n, \quad \forall e\in E, v\in V(e), n\in\{\mathrm{MPLS}\}, \tag{23}$$

$$\sum_{n\in\{\mathrm{WXC,MPLS}\}}\mu^v_n + \sum_{\substack{l'\in L(v)\\ l'\neq l}}\sigma^{e'k'}_{ekl'} \ge 1+M\cdot\left(\sigma^{e'k'}_{ekl}-1\right), \quad \forall e,e'\in E, e\neq e', k\in K(e), k'\in K(e'), v\in V, l\in L(v), \tag{24}$$

$$\sigma^{e'k'}_{ekl} \le \sum_{c\in C}\lambda^c_{ekl}, \quad \forall e,e'\in E, e\neq e', k\in K(e), k'\in K(e'), l\in L, \tag{25}$$

$$\sigma^{e'k'}_{ekl} \ge \sum_{c\in C}\lambda^c_{ekl} + \sum_{c\in C}\lambda^c_{e'k'l} - 1, \quad \forall e,e'\in E, e\neq e', k\in K(e), k'\in K(e'), l\in L, \tag{26}$$

$$\sum_{d\in D}\omega_{dek} \le M\cdot\sum_{p\in P(v)}\Psi^{vp}_{ek}, \quad \forall e\in E, k\in K(e), v\in V(e), \tag{27}$$

$$\sum_{p\in P(v)}\Psi^{vp}_{ek} \le 1, \quad \forall e\in E, k\in K(e), v\in V(e), \tag{28}$$

$$\sum_{e\in E}\sum_{k\in K(e)}\Psi^{vp}_{ek} \le 1, \quad \forall v\in V, p\in P(v), \tag{29}$$

$$\sum_{d\in D} b_d\cdot\omega_{dek} \le \tau^{vp} + M\cdot\left(1-\Psi^{vp}_{ek}\right), \quad \forall v\in V, p\in P(v), e\in E, k\in K(e), \tag{30}$$

$$\tau^{vp} \le \sum_{i\in\mathrm{PT}} pk_i\cdot\rho^{vp}_i, \quad \forall v\in V, p\in P(v), \tag{31}$$

$$\sum_{i\in\mathrm{PT}}\rho^{vp}_i \le 1, \quad \forall v\in V, p\in P(v), \tag{32}$$

$$\sum_{p\in P(v)}\tau^{vp} \le \sum_{j\in\mathrm{RT}} rk_j\cdot\pi^v_j, \quad \forall v\in V, \tag{33}$$

$$\sum_{p\in P(v)}\sum_{i\in\mathrm{PT}}\rho^{vp}_i \le \sum_{j\in\mathrm{RT}} rpk_j\cdot\pi^v_j, \quad \forall v\in V, \tag{34}$$

$$\sum_{j\in\mathrm{RT}}\pi^v_j \le 1, \quad \forall v\in V, \tag{35}$$

$$\alpha^v + M \cdot \left(1 - \sum_{n \in \{\text{WXC,MPLS}\}} \mu_n^v\right) \geq C_{\text{WXC}} + \varphi^v \cdot C_{\text{Trunk}}, \quad \forall v \in V, \tag{36}$$

$$\beta^v + M \cdot \left(1 - \sum_{n \in \{\text{MPLS}\}} \mu_n^v\right) \geq \sum_{p \in P(v)} \sum_{i \in \text{PT}} mpc_i \cdot \rho_i^{vp} + \sum_{j \in \text{RT}} rc_j \cdot \pi_j^v, \quad \forall v \in V. \tag{37}$$

The objective function (4) minimizes the network CAPEX. Constraints (5)–(7) compute the route and perform aggregation of demands through the virtual topology. Constraint (5) ensures that only one virtual link incident to source and destination nodes is used to transport the demand. Constraints (6) and (7) perform the routing and aggregation in intermediate nodes. Constraints (8)–(10) compute the route over the physical topology of those lightpaths transporting demands, and likewise constraints (5)–(7) do so for the demands over the virtual one. Constraints (11)–(14) perform spectrum allocation. Constraint (11) implements the spectrum continuity constraint ensuring that no more than one channel is allocated to one lightpath. Constraint (12) dimensions the size of the channel as a function of the aggregated bit-rate. Constraint (13) guarantees that every lightpath uses the same channel along its route. Constraint (14) ensures that each frequency slot is used by at most one lightpath. Constraints (15)–(17) take care of bit-rate-reach pair selection. Constraint (15) chooses a pair with enough bit-rate for the traffic to be transmitted, and constraint (16) ensures that the reach of that pair works for the length of the lightpath. Constraint (17) guarantees that only one pair is chosen.

Constraints (18)–(26) decide what equipment is installed in every location. Constraint (18) stores whether a fiber link is used or not, and constraint (19) stores the nodal degree of each location. Constraint (20) ensures that a location is equipped provided that some incident fiber link is used. Constraint (21) guarantees that only one type of node is selected to be installed in any location. Constraint (22) limits the nodal degree of any BV-WXC. Constraint (23) ensures that an IP/MPLS node (and its underlying BV-WXC) is installed in each location where any of the incident virtual links is used for transporting demands.

Constraints (24)–(26) decide whether a location must be equipped with a BV-WXC (with or without IP/MPLS functionality) or with a patch panel should fiber connectivity be the only functionality required among pairs of incident fiber links. Note that a BV-WXC must be installed provided that capacity to optically switch lightpaths among the incident fiber links in a location is needed (i.e., there exists a pair of lightpaths whose routes share only one incident fiber link at such particular location).

Constraints (27)–(32) deal with port slots. Constraint (27) ensures that any used lightpath is assigned to a port slot at its end nodes. Constraint (28) ensures that no more than one port is assigned at each end node of a lightpath. Constraint (29) ensures that a given port slot is not assigned to more than one lightpath. Constraint (30) stores the total amount of traffic transmitted through a given port slot. Constraint (31) equips port slots with BV-Ts of bit-rate sufficient to carry the amount of traffic assigned to the port slot. Constraint (32) ensures that only one BV-T is equipped in each port slot.

Constraints (33)–(35) manage IP/MPLS nodes. Constraint (33) equips an IP/MPLS node with switching capacity sufficient for the amount of traffic being switched at that location. Constraint (34) makes sure that the node type selected has sufficient port slots. Constraint (35) guarantees that only one node type is equipped at each location.

Finally, constraints (36) and (37) compute the cost of the BV-WXC and IP/MPLS nodes, respectively.

C. Complexity Analysis

The MIFO problem can be considered NP-hard since simpler multilayer network planning problems have been proved to be NP-hard (e.g., [22]). As to the MIFO problem size, the number of variables is $O(|E|^2 \cdot |K(e)|^2 \cdot |L| + |E| \cdot |K(e)| \cdot (|V| \cdot |P(v)| + |D| + |C| \cdot |L|)$, and the number of constraints is $O(|E|^2 \cdot |K(e)|^2 \cdot |L| + |E| \cdot (|K(e)| \cdot |V| \cdot |P(v)| + |D|) + |L| \cdot |S|)$. It is worth highlighting that the number of variables and constraints increase to approximately $3 \cdot 10^7$ and $6 \cdot 10^8$ for the networks presented in Section V.

Although the ILP can be solved for small instances (see Subsection IV.C), its exact solving becomes impractical for realistic backbone multilayer networks (under appreciable load) such as those described in Subsection V.A, even using commercial solvers such as CPLEX [23]. Thus, aiming at providing near-optimal solutions within reasonable computational effort, the next section presents a heuristic method to solve the MIFO problem.

IV. GRASP Heuristic Algorithm

In this section, we provide a detailed description of the GRASP heuristic algorithm that we have developed so as to efficiently solve the MIFO problem.

GRASP is an iterative two-phase metaheuristic method based on a multi-start randomized search technique. In the first phase, a greedy randomized feasible solution of the problem is generated through a *construction* algorithm. Then, in the second phase, a *local search* technique to explore an appropriately defined neighborhood is applied in an attempt to improve the current solution. These two phases are repeated until a stopping criterion (e.g., a number of iterations) is met, and once the procedure finishes the best solution found over all GRASP iterations is returned.

A. Construction Algorithm

The resolution of the MIFO problem primarily consists in routing, one-by-one, a set of demands over a virtual topology. For clarity, let us denote by $g(\cdot)$ the function that computes the CAPEX required to deploy the multilayer network. The CAPEX is computed using Eq. (4), and the specific network equipment cost values provided in Section V. The construction algorithm developed aims at generating demand orderings $O_x = \{d_1, \ldots, d_{|D|}\}$ that lead to the lowest possible CAPEX

values. Considering the given physical network topology and a full mesh virtual network computed on top, each demand $d \in D$ is associated to a sufficiently large set of pre-computed k_v shortest-path virtual routes $R_d = \{r_1, \ldots, r_k\}$; each route $r \in R_d$ is in turn associated to a set of k_o optical routes. Thus, in order to progressively generate an ordering vector, the incremental CAPEX cost ($c_d^* = \min\{c_d(r)\}, \forall r \in R_d$) of routing each demand is computed so that the demand leading to the smallest incremental cost $d^* = \min_{d \in D}\{c_d(r)\}$ is added to O_x. Note that $c_d(r)$ corresponds to the incremental cost of routing demand d through the cheapest route $r^* \in R_d$. For the sake of clarity, in the GRASP-specific pseudo-codes shown in Procedures 1, 3, and 4, we assume that function $g(\cdot)$ is able to compute the CAPEX only receiving as input parameter ordering O_x. A detailed explanation of the CAPEX computation is provided in Procedure 2.

Procedure 1 Sample Greedy Construction

INPUT: $D, R_d, \forall\, d \in D, \tau$;
OUTPUT: $O_x, g(O_x)$;
1: Initialize $O_x \leftarrow \emptyset$ and candidate set: $Q \leftarrow D$;
2: **while** $\mathcal{Q} \neq \emptyset$ **do**
3: Randomly sample $\min\{\tau \cdot |D|, |Q|\}$ elements from Q and put them in RCL;
4: Evaluate the minimum incremental cost c_d^*, $\forall\, d \in RCL$;
5: Select $d^* = \text{argmin}\{c_d^* : d \in RCL\}$;
6: $O_x \leftarrow O_x \cup \{d^*\}$;
7: $Q \leftarrow Q \backslash \{d^*\}$;
8: **end while**
9: Compute $g(O_x)$;

In this work, given both the fact that computing $c_d(r), \forall r \in R_d$, $\forall d \in D$, is a time-consuming task and that the size of the real-sized traffic and network instances is usually really large, we have implemented the sample greedy (SG) construction method [14]. In this alternative construction algorithm, the greedy and randomization rules are balanced in an attempt to lower the worst-case complexity of the common greedy randomized (GR) construction [14], which in order to fill the *restricted candidate list* (RCL) evaluates at each step all possible candidates. In contrast, as illustrated by the pseudo-code in Procedure 1, SG only samples a subset of the candidates at each iteration, and then the element providing the best incremental cost (d^*) is added to the current solution. The percentage of elements evaluated to fill the RCL is controlled by the input parameter $\tau \in [0,1]$. Note that parameter τ here is used to balance between greediness and randomness in the construction, with larger τ values leading to greedier solutions and higher time consumption.

To evaluate cost c_d (i.e., the CAPEX) for routing each demand d through any virtual route $r \in R_d$, the heuristic algorithm proposed aims at determining the type of node to be deployed at each location as well as the type and number of BV-Ts to be installed. To this end, the steps detailed in Procedure 2 are executed. First, in line 1, demand d is added to all virtual links belonging to virtual route r. Then, for each virtual link e in the network, the loop in lines 2–6 determines the number and type (Gb/s) of the candidate lightpaths (CLs) that have to be established between each pair of locations in the network. The term CL here is used to emphasize that it is not until the node type to be installed at each location is known that the lightpaths are actually established. After

Procedure 2 Construct multilayer network

INPUT: V, E, d, r;
OUTPUT: Multilayer network infrastructure;
1: Associate d to all virtual links $e \in r$;
2: **for all** $e \in E$ **do**
3: Take set of demands D_e using e (if any);
4: Groom demands in D_e and determine the number and type of candidate lightpaths (CLs) required;
5: Associate CL to both $v \in V(e)$;
6: **end for**
7: **for all** $v \in V$ **do**
8: According to the CLs ending or originating at v and the demands they groom, determine the type of node to be installed (IP/MPLS, BV-WXC, Patch panel or Empty) and type and number of BV-Ts required;
9: **end for**
10: Compute COST_{FO} according to the installed BV-Ts, which determine the lightpaths actually established in the network;
11: Compute CAPEX using $g(V, \text{COST}_{\text{FO}})$;

grooming the demands into CLs, the number of contiguous FSs required by each CL is obtained. Then, an efficient first-fit RSA algorithm is run in order to allocate spectrum resources along all optical links in route $k_o = 1$ supporting e. Specifically, we model optical links as binary vectors ($x[i]$), where each position represents one FS ($x[i] = 1$ (used) or 0 (free)). Hence, given the number of contiguous FSs required, a logic *and* operation considering all optical links supporting e is computed to find all the candidate set of contiguous FSs where the groomed demand can be allocated. Among them, we select the set of FSs to be used in a first-fit basis. If no candidate set of FSs is found, then $k_o = 2$ is attempted. As mentioned in Section I, this strategy is similar to the fixed-alternate and first-fit frequency allocation algorithm (see, e.g., [10]). The main difference lies in the fact that in this work the order in which these demands are served is controlled by the proposed GRASP methodology.

The subsequent *for* loop (lines 7–9) determines the equipment to be installed at each location. Finally, according to the BV-Ts deployed, the algorithm is able to determine the actual lightpaths established and the associated cost for using the fiber (COST_{FO}). Hence, in line 11, the CAPEX can be easily computed by applying $g(\cdot)$. Note that once the cheapest route r^* is found (and hence so is d^*), d^* is routed through r^*, and the set of virtual links is updated accordingly to keep track of the demands already served. As the loop in Procedure 1 progresses, the number of demands supported by the set of virtual links E (input for the algorithm in Procedure 2) increases, and so does the size and CAPEX of the multilayer network.

In line 8 in Procedure 2, given the CLs ending or originating at node $v \in V$, the functionality required at v can be determined. For instance, let us assume that v has only one originating lightpath (l_o) and one ending lightpath (l_e), none of the demands groomed in such lightpaths is originating or ending at v, and both lightpaths groom exactly the same demands; this means that a patch panel can be placed at v, as only fiber connectivity is required. In contrast, assuming that another lightpath ($l_{e'}$) is also ending at v through the same input port as l_e, none of the demands it supports ends at v, and $l_{e'}$ has its exact replica in one of the output ports (i.e., carrying the same groomed demands and using the same FSs (same channel)), then a BV-WXC needs to be installed, as

only optical switching functionality is required. Finally, if any of the demands in such lightpaths ends or originates at v, or if any of the ending lightpaths does not have its exact replica in an originating one, then IP/MPLS equipment needs to be installed, as electronic processing of the signals is required. Note that, if no lightpaths end or originate at v, the location is left empty.

B. Local Search Algorithm

Since a feasible solution to the problem (O_x) output by Procedure 1 has no guarantee of being locally optimal, let us denote by $N_q(O_x)$ the set of solutions in the q_{th} neighborhood structure of O_x. Thus, assuming an order $O_x = \{d_1,\ldots,d_i,\ldots,d_j,\ldots,d_{|D|}\}$, we define the neighbor of this ordering as an ordering in which d_i swaps its position with d_j. In order to generate a random neighbor in the first neighborhood of O_x (i.e., $N_1(O_x)$), we choose pivots d_i and d_j uniformly among the $|D|$ demands. Hence, creating a N_q neighbor implies that this random swap of demands is performed q times. In this work, we have adopted the variable neighborhood descent (VND) [24] algorithm to perform the local search within the GRASP methodology. Specifically, VND explores a limited number of neighborhood structures ($mxStr$), by uniformly sampling a number of neighbors ($mxSam$) in each of them. Starting with N_1, VND performs local search until no further improvement is found. The VND pseudo-code is shown in Procedure 3.

Procedure 3 Variable neighborhood descent

INPUT: $O_x, mxStr, mxSam$;
OUTPUT: $O_{\text{BEST}}, g(O_{\text{BEST}})$;
Initialize $O_y \leftarrow O_x$, $O_{\text{BEST}} \leftarrow O_x$ and $k \leftarrow 1$;
while $k < mxStr$ **do**
  Randomly sample $mxSam$ elements in $N_k(O_y)$ and let O'_y be the best solution obtained;
  if $g(O'_y) < g(O_y)$ **then**
    $O_{\text{BEST}} \leftarrow O'_y$;
    $O_y \leftarrow O'_y$;
    $k \leftarrow 1$;
  else
    $k \leftarrow k+1$;
  end if
end while

C. GRASP Algorithm

Finally, the pseudo-code for the GRASP algorithm is illustrated in Procedure 4, where it is possible to observe that the multi-start phase (i.e., SG followed by VND) is executed for $mxIter$ iterations.

The performance of the proposed GRASP methodology has been compared against the ILP model described in Section III. To be able to solve the ILP model, however, we had to consider a size-constrained multilayer network (e.g., limiting the size of the virtual topology) and a very small number of demands for each experiment. In all the experiments performed, the GRASP heuristic was able to provide a much better trade-off between optimality and computation time due to the high difficulty in solving the model. Although for these preliminary experiments the input GRASP parameters were manually tuned, for the realistic network scenarios considered in this study a more advanced approach was employed, as explained in Section V.

Procedure 4 GRASP algorithm

INPUT: $D, R_d, \forall\, d \in D, \tau, mxStr, mxSam, mxIter$;
OUTPUT: $O_{\text{BEST}}, g(O_{\text{BEST}})$;
Initialize $O_{\text{BEST}} \leftarrow \emptyset$, $i \leftarrow 0$;
while $i < mxIter$ **do**
  $O_x \leftarrow SG(D, R_d, \forall\, d \in D, \tau)$;
  $O'_x \leftarrow VND(O_x, mxStr, mxSam)$;
  if $g(O'_x) < g(O_{\text{BEST}})$ **then**
    $O_{\text{BEST}} \leftarrow O'_x$;
  end if
  $i \leftarrow i+1$;
end while

V. Illustrative Numerical Results

In this section, we first present the network scenarios that we consider in order to carry out our experiments. Second, we perform the tuning of the input parameters required to execute the GRASP heuristic, and finally we solve the MIFO problem considering a set of realistic network and traffic instances.

A. Network Scenario

In order to conduct all the experiments, we consider the three optical network topologies shown in Fig. 2; these are the 21-node Spanish Telefónica (TEL) topology, the 20-node British Telecom (BT) topology, and the 21-node Deutsche Telekom (DT) topology. In these networks, we assume that $V_v = V$, that is, that any location can host an IP/MPLS node. Besides, only those locations in blue in Fig. 2 can be the source or destination of IP/MPLS demands (as explained in Section II). The remaining locations (i.e., the intermediate locations) will be equipped according to the MIFO problem solution.

As to the traffic profiles (TPs) considered, we make use of three TPs as reported in Table II. Although each TP injects into the network the same average amount of Tb/s, the traffic scenarios proposed feature lightly loaded demands in TP-1 (only 24.1 Gb/s on average), medium load demands (52.0 Gb/s) in TP-2, and high bit-rate demands in TP-3 (80 Gb/s). Hence, the number of demands served decreases substantially from TP-1 to TP-3 in order to keep the total volume of Tb/s injected constant. These TPs are a realistic representation of the expected evolution of bandwidth necessities for the years to come in increasing order. Note that in this study we do not consider the expected increase in the total traffic volume, as our goal is to determine what the optimal slot width is given the expected increase in the average demand bit-rate. In our experiments, the optical spectrum width used was in line with the demands to be served in each TP. To be exact, using 2 THz we corroborated that for all traffic representations executed a feasible solution could be found. Table III (IP/MPLS nodes) and Table IV (BV-Ts) provide the characteristics of the network equipment considered as well as their value in cost units (c.u.) that we use to compute the CAPEX. All these values have been obtained from discussions currently being held within the STRONGEST project [25].

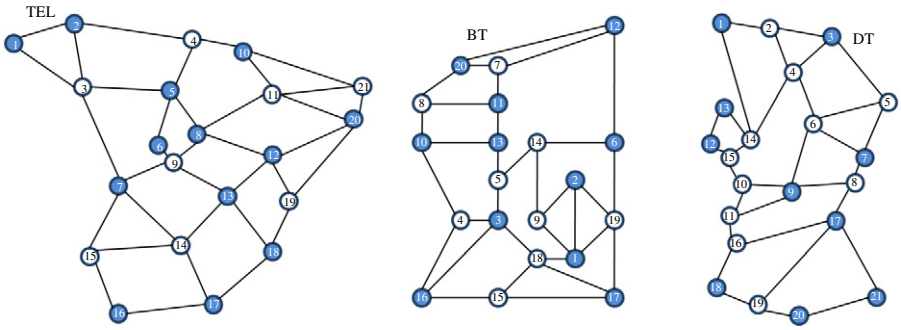

Fig. 2. (Color online) Optical network topologies considered: the 21-node Spanish Telefónica (TEL), the 20-node British Telecom (BT), and the 21-node Deutsche Telecom (DT).

TABLE II
TRAFFIC PROFILES (TPS) ANALYZED

TP	Average bit-rate (Gb/s)	Demands (%) 10 Gb/s	40 Gb/s	100 Gb/s	400 Gb/s
TP-1	24.1	80	13.4	5.4	1.3
TP-2	52	40	40	16	4
TP-3	80	0	66.7	26.7	6.7

TABLE III
COST AND FEATURES OF IP/MPLS NODES

Node	Class 1	Class 2	Class 3	Class 4	Class 5
Capacity (Gb/s)	160	320	640	1280	2560
Maximum ports	4	8	16	32	64
Cost (c.u.)	9	13.5	19.5	67.5	150.57

TABLE IV
COST AND REACH OF BV-TS

BV-T	10 Gb/s	40 Gb/s	100 Gb/s	400 Gb/s
Reach (km)	2500	2000	1000	400
Cost (c.u.)	2.5	7.625	20.625	65.625

In addition, we assume an optical amplifier cost of 5 c.u., and $C_{\mathrm{FO}} = 0.02$, that is, the cost per km and GHz of using the already deployed optical fiber. As mentioned in Section II, we consider QPSK ($B_{\mathrm{mod}} = 2$) as the modulation format. Note that, considering QPSK and the network topologies shown in Fig. 2, it can be assumed that the number of cascaded BV-WXCs traversed by a demand does not need to be limited [2]. In order to route the demands, a set of k shortest paths is pre-computed over both the physical (k_o) and virtual (k_v) network topology. To this end, we implemented Yen's algorithm as proposed in [26]. Specifically, we set k_o and k_v to a maximum of 200 and 400 shortest paths, respectively.

B. GRASP Parameter Tuning

In order to find appropriate values for the input parameters of the GRASP procedure, we make use of the automatic biased random-key genetic algorithm (BRKGA) tuning for GRASP heuristics as proposed in [27]. The parameters that need to be adjusted are τ in the SG construction algorithm and both $mxStr$ and $mxSam$ for the VND local search heuristic. Thus, the chromosome used to run BRKGA is defined by these three parameters. We test the following values for each of them: $\tau = \{0.1, 0.2, 0.3, 0.4\}$, $mxStr = \{5, 10, 15\}$, and $mxSam = \{10, 15, 20\}$. To run BRKGA, we use the same approach and input parameter values as in [13]. BRKGA tuning is run considering five reduced-size traffic instances for each TP and network, and as a result a combination of parameters is obtained for each of them. The parameters found to run GRASP are provided in Table V.

TABLE V
GRASP AUTOMATICALLY TUNED PARAMETERS

Network	τ	$mxStr$	$mxSam$
TEL	0.2	5	15
BT	0.3	10	10
DT	0.3	5	15

C. CAPEX Using Relative (Grid-Dependent) BV-WSS Costs

Next, we solve the MIFO problem with the aim of finding, given a target CAPEX investment and a set of relative cost values for the different BV-WSSs, the maximum affordable cost for each (grid-dependent) BV-WSS. Although the actual cost for these enhanced optical devices (also involving higher costs due to a more complex control plane) is still not available, we assume that the finer the grid, the higher the relative cost for a BV-WSS device should be.

In Fig. 3, we provide, for each network topology, the traffic profile (TP), the frequency grid, and the network CAPEX for the MIFO problem solution. Note that the CAPEX here only accounts for the network equipment costs (i.e., Eq. (2)). Each of the points in the plots corresponds to an average over 10 independent runs (each lasting for 40 iterations) of the GRASP heuristic algorithm. For the sake of a comprehensive analysis, we consider two traffic scenarios for each TP; these are a highly loaded scenario (4.5 Tb/s are injected into the network) and a medium one (3.5 Tb/s). Thus, out of the 10 runs, 5 correspond to the highly loaded scenario and 5 to the medium one.

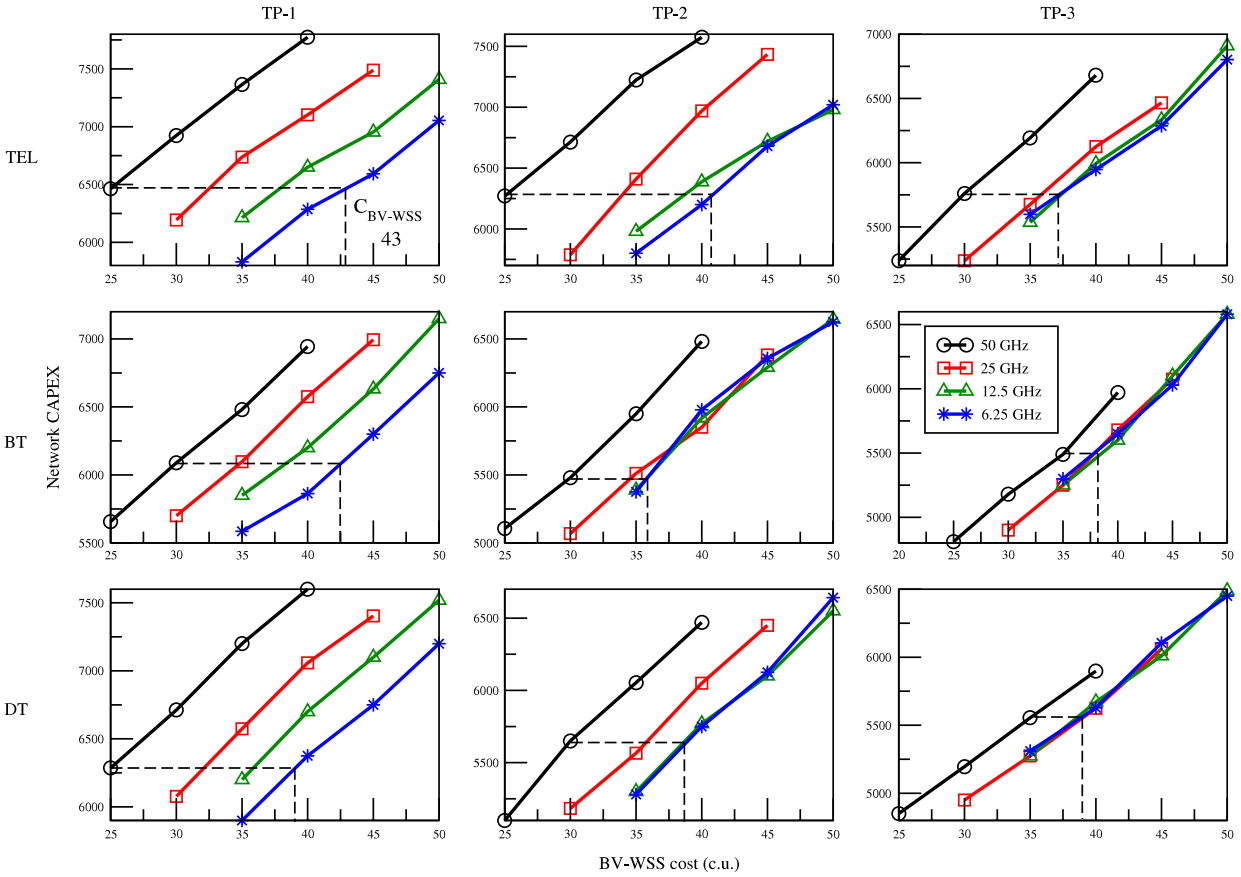

Fig. 3. (Color online) Network CAPEX (IP/MPLS and optical equipment cost) as a function of the relative cost for one BV-WSS. The three network topologies are analyzed under the four different slot widths.

TABLE VI
AVERAGE BV-T NUMBER (#) AND BIT-RATE (Gb/s)

		#			Gb/s		
Network	Grid	TP-1	TP-2	TP-3	TP-1	TP-2	TP-3
TEL	50	158	148	119	64	70	70
	25	190	179	118	50	49	67
	12.5	229	219	117	37	39	66
	6.25	277	260	118	30	32	66
BT	50	136	121	111	55	59	64
	25	170	150	112	42	47	63
	12.5	215	160	111	32	41	58
	6.25	255	164	110	26	39	57
DT	50	147	117	115	59	58	62
	25	183	140	117	49	50	61
	12.5	235	157	116	41	45	60
	6.25	257	170	117	31	41	61

TABLE VII
AVERAGE REDUCTION PER GRID IN NODE SWITCHING CAPACITY (SW) AND FLOW SWITCHED (FS) (WITH RESPECT TO THE 50 GHz GRID)

		SW (%)			FS (%)		
Network	Grid	TP-1	TP-2	TP-3	TP-1	TP-2	TP-3
TEL	25	13	11	8	10	8	4
	12.5	20	13	8	16	9	4
	6.25	24	13	8	24	11	4
BT	25	5	4	1	5	5	1
	12.5	8	7	2	7	7	2
	6.25	14	7	2	14	8	3
DT	25	4	6	1	4	12	1
	12.5	11	10	1	11	13	2
	6.25	17	14	1	17	14	2

The plots in Fig. 3 clearly illustrate the effectiveness of narrower grids in grooming data directly at the optical layer, thus reducing the network CAPEX. Besides, such a positive effect is clearly dependent on the TP considered. For TP-1, one can observe that the introduction of finer grids allows for the spectrum to be better exploited, and hence to achieve further benefit. In TP-2, by contrast, the 6.25 GHz grid provides the same performance as the 12.5 GHz in both the TEL and DT networks, and the 25 GHz in the BT network. Eventually, in TP-3, the main benefit is obtained just by considering a 25 GHz grid.

Complementing these results, Table VI reports the average number and bit-rate of the installed BV-Ts, and Table VII provides the average reduction (with respect to the 50 GHz grid) in both IP/MPLS node switching capacity and actual amount of traffic switched (flow switched). As expected, these values are strongly dependent on both the frequency grid and TP evaluated. As anticipated in Section II, and as long as the TP analyzed allows for it, the use of finer frequency grids

TABLE VIII
AVERAGE BV-WSS AFFORDABLE COST INCREMENT PER FREQUENCY GRID (%)

Grid	TP-1	TP-2	TP-3	Average
25	25.6	27.3	16.6	23.2
12.5	41.3	36.1	23	33.5
6.25	57.6	38.9	23.4	39.9

entails a higher number of BV-Ts due to the more fragmented spectrum, which eventually results in a different grooming of demands into lightpaths (according to the mapping shown in Table I and the equipment costs provided in this section). However, this increase comes at the benefit of having a considerably much lower average bit-rate per BV-T, a fact which leads to lower switching capacity, and therefore, to cheaper IP/MPLS equipment.

Finally, in order to estimate the maximum affordable cost increment for a BV-WSS in the 6.25 GHz grid, we use as a benchmark reference a BV-WSS cost in the 50 GHz grid (see dotted lines in Fig. 3). In the TEL network under TP-1, the cost of the BV-WSSs can be, for the same network CAPEX, as high as 43 c.u., that is, 72% more expensive than the one used in the 50 GHz grid (25 c.u.). However, when the on-average bit-rate of the demands increases in both TP-2 and TP-3, the cost of a BV-WSS decreases to about 41 c.u. (64%) and 37 c.u. (23%), respectively.

In Table VIII, the average BV-WSS affordable cost increment provided by each frequency grid is reported. In light of these results, which represent an average over the three network topologies, it is clear that from a temporal perspective given by the on-average bit-rate of demands, high cost increments can be assumed for a 6.25 GHz grid BV-WSS in the near future (57.6%). However, considering the expected traffic evolution, which for the long term estimates a TP similar to TP-3 analyzed in this paper, these investments will not be profitable. Therefore, it can be concluded that investments in flexgrid optical networks using the 12.5 GHz or even the 25 GHz grid (considering the increased management complexity of the network in finer frequency grids) are cheaper in the short term and are more appropriate for medium-term and long-term scenarios.

VI. CONCLUSIONS

This paper has addressed the design of a multilayer IP/MPLS-over-flexgrid network. To this end, an ILP formulation has been presented and, given its complexity, a GRASP metaheuristic has been developed. Through extensive numerical experiments, we have analyzed the cost implications that the frequency grid (slot width) has on this emerging multilayer network planning problem. For the sake of a comprehensive study, we have considered a set of realistic network topologies, equipment costs, and traffic instances.

The results have shown that the benefits that can be achieved through the use of finer slot widths are strongly dependent on the actual traffic profile (TP) under which the network is operating. Whilst investments in costly BV-WSS (finer grid) devices are very well motivated under traffic conditions reporting a high number of light bit-rate demands, which represent short-term traffic scenarios, they do not seem profitable in the long term, where a reduced number of higher bit-rate demands are expected. Consequently, this study reports both the 12.5 GHz and the 25 GHz slot widths as potential candidates for the deployment of future multilayer networks based on flexgrid technology.

ACKNOWLEDGMENTS

The research leading to these results has received funding from the European Community's Seventh Framework Programme FP7/2007-2013 under grant agreement no. 247674 (STRONGEST Project). Moreover, it was supported by the Spanish Ministry of Science through the FPU Program and the DOMINO Project (TEC2010-18522). This paper was presented in part at OFC/NFOEC 2012 [28].

REFERENCES

[1] M. Jinno, H. Takara, B. Kozicki, Y. Tsukishima, Y. Sone, and S. Matsuoka, "Spectrum-efficient and scalable elastic optical path network: Architecture, benefits, and enabling technologies," *IEEE Commun. Mag.*, vol. 47, no. 11, pp. 66–73, 2009.

[2] M. Jinno, B. Kozicki, H. Takara, A. Watanabe, Y. Sone, T. Tanaka, and A. Hirano, "Distance-adaptive spectrum resource allocation in spectrum-sliced elastic optical path network," *IEEE Commun. Mag.*, vol. 48, no. 8, pp. 138–145, 2010.

[3] Finisar, "Programmable narrow-band filtering using the WaveShaper 1000E and WaveShaper 4000E," *White Paper*, 2011 [Online]. Available: http://www.finisar.com.

[4] *ITU-T Recommendation G.694.1*, "Spectral grids for WDM applications: DWDM frequency grid," 2012 [Online]. Available: http://www.itu.int/rec/T-REC-G.694.1-201202-I/en.

[5] K. Christodoulopoulos, I. Tomkos, and E. Varvarigos, "Elastic bandwidth allocation in flexible OFDM based optical networks," *J. Lightwave Technol.*, vol. 29, no. 9, pp. 1354–1366, May 2011.

[6] Y. Wang, X. Cao, and Y. Pan, "A study of the routing and spectrum allocation in spectrum-sliced elastic optical path networks," in *IEEE Int. Conf. on Computer Communications (INFOCOM)*, Apr. 2011.

[7] L. Velasco, M. Klinkowski, M. Ruiz, and J. Comellas, "Modeling the routing and spectrum allocation problem for future elastic optical networks," *Photonic Network Commun.*, 2012 [Online]. Available: http://dx.doi.org/10.1007/s11107-012-0378-7.

[8] X. Wan, L. Wang, N. Hua, H. Zhang, and X. Zheng, "Dynamic routing and spectrum assignment in flexible optical path networks," in *Optical Fiber Communication Conf. and the Nat. Fiber Optic Engineers Conf. (OFC/NFOEC)*, Mar. 2011, JWA55.

[9] K. Christodoulopoulos, I. Tomkos, and E. Varvarigos, "Dynamic bandwidth allocation in flexible OFDM-based networks," in *Optical Fiber Communication Conf. and the Nat. Fiber Optic Engineers Conf. (OFC/NFOEC)*, Mar. 2011, OTuI5.

[10] M. Klinkowski and K. Walkowiak, "Routing and spectrum assignment in spectrum sliced elastic optical path network," *IEEE Commun. Lett.*, vol. 15, no. 8, pp. 884–886, Dec. 2011.

[11] J. Santamaría, O. Cordón, S. Damas, R. Martí, and R. Palma, "GRASP and path relinking hybridizations for the point matching-based image registration problem," *J. Heuristics*, vol. 18, no. 1, pp. 169–192, 2012.

[12] H. Höller, B. Melián, and S. Voß, "Applying the pilot method to improve VNS and GRASP metaheuristics for the design of SDH/WDM networks," *Eur. J. Oper. Res.*, vol. 191, no. 3, pp. 691–704, Dec. 2008.

[13] O. Pedrola, M. Ruiz, L. Velasco, D. Careglio, O. González de Dios, and J. Comellas, "A GRASP with path-relinking heuristic for the survivable IP/MPLS-over-WSON multi-layer network optimization problem," *Comput. Oper. Res.*, 2012 [Online]. Available: http://dx.doi.org/10.1016/j.cor.2011.10.026.

[14] M. G. C. Resende and C. C. Ribeiro, "Greedy randomized adaptive search procedures: Advances and applications," in *Handbook of Metaheuristics*, M. Gendreau and J. Y. Potvin, Eds., 2nd ed. Springer Science+Business Mediapp, 2010, pp. 29–63.

[15] O. Ribal and A. Morea, "Cost-efficiency of mixed 10-40-100 Gb/s networks and elastic optical networks," in *Optical Fiber Communication Conf. and the Nat. Fiber Optic Engineers Conf. (OFC/NFOEC)*, Mar. 2011, OTuI4.

[16] M. Ruiz, O. Pedrola, L. Velasco, D. Careglio, J. P. Fernández-Palacios, and G. Junyent, "Survivable IP/MPLS-over-WSON multi-layer network optimization," *J. Opt. Commun. Netw.*, vol. 3, no. 8, pp. 629–640, Aug. 2011.

[17] K. Zhu and B. Mukherjee, "Traffic grooming in an optical WDM mesh network," *IEEE J. Sel. Areas Commun.*, vol. 20, no. 1, pp. 122–133, Jan. 2002.

[18] B. Chen, G. Rouskas, and R. Dutta, "Clustering methods for hierarchical traffic grooming in large-scale mesh WDM networks," *J. Opt. Commun. Netw.*, vol. 2, no. 8, pp. 502–514, Aug. 2010.

[19] S. Koo, G. Sahin, and S. Subramaniam, "Dynamic LSP routing in IP/MPLS-over-WDM networks," *IEEE J. Sel. Areas Commun.*, vol. 24, no. 12, pp. 45–55, Dec. 2006.

[20] H. Höller and S. Voß, "A heuristic approach for combined equipment-planning and routing in multi-layer SDH/WDM networks," *Eur. J. Oper. Res.*, vol. 171, no. 3, pp. 787–796, June 2006.

[21] M. Pióro and D. Medhi, *Routing, Flow, and Capacity Design in Communication and Computer Networks*. Morgan Kaufmann Publishers, 2004.

[22] X. Zhang, F. Shen, L. Wang, S. Wang, L. Li, and H. Luo, "Two-layer mesh network optimization based on inter-layer decomposition," *Photonic Network Commun.*, vol. 21, no. 3, pp. 310–320, 2011.

[23] IBM ILOG CPLEX, 2012 [Online]. Available: http://www-01.ibm.com/software/integration/optimization/cplex/.

[24] P. Hansen and N. Mladenovic, "Variable neighborhood search: principles and applications," *Eur. J. Oper. Res.*, vol. 130, no. 3, pp. 449–467, May 2001.

[25] STRONGEST: Scalable, Tunable and Resilient Optical Networks Guaranteeing Extremely-high Speed Transport, 2012 [Online]. Available: http://www.ict-strongest.eu/.

[26] E. Martins and M. Pascoal, "A new implementation of Yen's ranking loopless paths algorithm," *4OR: Q. J. Oper. Res.*, vol. 1, no. 2, pp. 121–133, 2003.

[27] P. Festa, J. F. Gonçalves, M. G. C. Resende, and R. M. A. Silva, "Automatic tuning of GRASP with path-relinking heuristics with a biased random-key genetic algorithm," in *Experimental Algorithms* (Vol. 6049 of Lecture Notes in Computer Science). 2010, pp. 338–349.

[28] O. Pedrola, A. Castro, L. Velasco, D. Careglio, J. P. Fernández-Palacios, and G. Junyent, "CAPEX study for grid dependent multi-layer IP/MPLS-over-EON using relative BV-WSS costs," in *Optical Fiber Communication Conf. and the Nat. Fiber Optic Engineers Conf. (OFC/NFOEC)*, Mar. 2012, NTu2J.7.